2014 ASIA-PACIFIC SOLAR RESEARCH CONFERENCE

Peer Reviewed
2014 Solar Research Conference

Simulation results of a high-temperature solar-cooling system with different control strategies

Sergio Pintaldi[1,4], Ali Shirazi[2], Subbu Sethuvenkatraman[4], Stephen White[4], Gary Rosengarten[1], Robert A Taylor[2,3]

[1]*School of Aerospace, Mechanical and Manufacturing Engineering, Royal Melbourne Institute of Technology, 115 Queensberry St, Carlton, Australia*
[2]*School of Mechanical and Manufacturing Engineering, The University of New South Wales, Kensington, New South Wales, Australia*
[3]*School of Photovoltaic & Renewable Energy Engineering, The University of New South Wales, Kensington, New South Wales, Australia*
[4]*Energy Flagship, Commonwealth Scientific and Industrial Research Organisation, 10 Murray Dwyer Circuit, Steel River Industrial Park, Newcastle, Australia*
E-mail: sergio.pintaldi@csiro.au

Abstract

High-temperature absorption chillers (double-effect and triple-effect) have a higher coefficient of performance (COP) than single-effect chillers. This can reduce the collector's footprint and cost in a solar-cooling plant. Though single-effect, absorption chiller-based solar-cooling systems have been studied for the past 20 years, very little information is available on the performance benefits of high-temperature solar-cooling systems. The behaviour of a solar-driven, triple-effect absorption chiller with thermal storage, when serving an office building load, have been analysed in this paper. Characteristic equations for the triple effect chiller have been developed from their operating performance data. The effect of different control strategies and design parameters on the annual performance of the system have been captured in this paper. These results indicate that it is possible to achieve very high solar fractions (> 0.9) by choosing the right size of system components and a suitable control strategy.

1. Introduction

Various design options for solar driven air conditioning systems exist (Pintaldi et al., 2015). These include choices related to component sizing, (collector and storage size) integration of backup heat source and control strategy. These choices are also load dependent. Considering the multiple variables involved, system level simulations have been used by researchers to identify a suitable system layout for a given application. The Transient System Simulation TRNSYS (Solar Energy Laboratory, University of Wisconsin, 2011) has been widely used by researchers as a tool during these evaluations (e.g. (Al-Alili et al., 2012; Eicker and Pietruschka, 2009)). Eicker and Pietruschka have used TRNSYS based simulations to evaluate design and performance of solar air conditioning systems for office buildings. They used single effect absorption chillers in their studies to characterise energy and economic benefits. Al-Alili et al. have optimized a solar powered absorption system for Abu Dhabi's weather conditions using TRNSY and GenOpt optimization algorithm. Hang et al (Hang et al., 2013) have used multi objective optimization techniques to identify optimum solar absorption cooling and heating system configuration for medium sized office buildings in various locations of USA. Solar cooling system configurations for various other locations have also been studied through simulations (Mateus and Oliveira, 2009; Tsoutsos et al., 2010).

However, literature with system level benefits of high temperature solar cooling systems is very limited. Qu et al. (Qu et al., 2010) have analysed the benefits of a double effect chiller-based system for a building using system level simulations. There is no published literature on the optimization of a solar cooling system utilizing triple effect absorption chillers. Thus, a model to capture the performance of a triple effect chiller has been developed and the approach is presented in this paper. Utilizing this model, system level benefits of a triple effect solar cooling system configuration for an office building are evaluated in this paper.

2. Model description and simulation methodology

The solar cooling system configuration is shown in Figure 1. It consists of parabolic trough collectors for generation of high temperature heat (> 200°C), a backup heat source and a storage tank to aid in solar intermittency and to serve as a backup during non-solar periods. The triple-effect absorption chiller with cooling tower makes up the cooling generation system. This layout is simulated using TRNSYS. Details of component specification in the model are provided in Table 1. As a detailed validation of the model is not possible (due to lack of test data), sanity checks such as chiller energy balance and total system energy balance were monitored throughout the simulations.

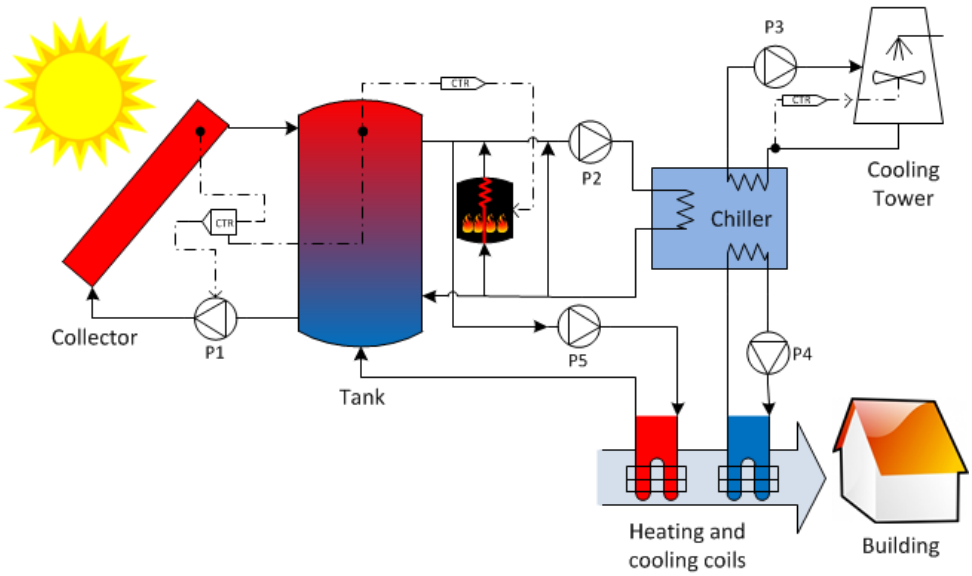

Figure 1. Simulated solar-cooling layout

2.1. Building load

The building model used in this study represents a typical office building, located in medium and large Australian cities, and falling under building category A of the Australian Building Codes Board[1]. The building has a fully enclosed area of ~1000 m^2; the dimensions of the sides are 31.6 x 31.6 m, and the floor-to-ceiling height is 2.7 m.

[1] ACADS-BSG Pty Ltd, Elms Consulting Engineers (May 2002) ABCB Energy modelling of office buildings for climate zoning, stages 1, 2 & 3, p. 2; ABCB www.abcb.gov.au; Major Initiatives > Energy Efficiency > Multi-Residential, Commercial and Public Buildings > Archived Documents (www.abcb.gov.au/major-initiatives/energy-efficiency/multi-residential-commercial-and-public-buildings).

The building walls and fabric were designed to meet the minimum requirements provided by the Building Code of Australia. The internal loads were based on 100-person occupancy and a low infiltration rate (0.25 air changes/h). Loads associated with lighting and equipment were included in the model. Temperature set-points for cooling and heat mode operations were 24 °C and 20 °C, respectively. To meet the comfort requirements, the operating time for the air-conditioning system was set between 0700 and 1800 hours.

These conditions resulted in an annual cooling and heating demands of 15 MWh and 0.310 MWh, respectively, for a building located in Newcastle, Australia.

Table 1 summarises the main parameters and coefficients used in the simulations. The chiller model and the system controllers are discussed in Section 2.2 and Section 3, respectively.

Table 1. Description of the main system component parameters

Component	Description
Weather data	Newcastle, Williamtown Airport
Solar collector	Efficiency parameters for the solar collector are η_0 = 0.689, a_1 = 0.36W/m^{2}K, a_2 = 0.0011W/m^{2}K^2. Water is the working fluid in the collector loop.
Thermal store	Hot storage tank of height-to-diameter ratio of 3.5. Overall heat loss coefficient set to 0.83 W/m^{2}K.
Back-up system	Instantaneous gas burner with a set-point temperature of 220 °C. The back-up position can be set to series or parallel.
Cooling tower	Wet cooling tower in a counter-flow configuration. A controlled, variable-speed fan maintained the outlet temperature of cooling water at a constant value of 32 °C.
Pumps	The system used five pumps, as shown in Figure 1. The solar pump (P1) worked in variable-speed mode or fixed-speed mode depending on the controller type. Details of these controls are explained in Section 3. All other pumps (P2–P5) operated in ON–OFF mode.

2.2. Triple-effect absorption chiller model

Thermodynamic models for absorption chillers are complex to implement and computationally expensive for detailed annual energy performance simulations. Thus, various empirical and semi-empirical modelling approaches for predicting absorption chiller performance have been documented (Labus et al., 2013; Puig-Arnavat et al., 2010). The current model is based on the characteristic temperature function ΔΔT, as described by Kühn and Ziegler (2005). The energy balance equations are:

$$Q_{AC} = Q_E + Q_G + Q_{aux} \quad (1)$$

$$COP = \frac{Q_E}{Q_G + Q_{aux}} \quad (2)$$

$$Q = \dot{m} \cdot c_p (T_o - T_i) \quad (3)$$

The expression of the evaporator and generator power is:

$$Q = s \cdot \Delta\Delta t + r \quad (4)$$

Where the characteristic temperature function is:

$$\Delta\Delta t = t_G + a \cdot t_{AC} + e \cdot t_E \quad (5)$$

The subscripts are: *G* for chiller generator, *AC* for absorber and condenser, *E* for evaporator, *aux* for auxiliary, *o* for output, *i* for input, *T* for temperature and *t* for average temperature

between the inlet and the outlet. The model has been calibrated using triple-effect, hot-water-fired absorption chiller data provided by Thermax (Thermax and CSIRO, 2014). Statistical analysis was performed according the 'second method' described by Puig-Arnavat et al. (2010) and *Microsoft Excel* was used for multi-variable regression analysis of the cooling capacity. The characteristic temperature function parameters obtained from the above process were then used for a mono-variable regression analysis of the generator capacity to obtain the generator parameters of Equation 4. Table 2 summarises the coefficients used in Equations 3–5.

Table 2. Triple-effect absorption chiller parameters

Characteristic equation parameters	Value	Additional parameters	Value
a	–2.63156	Chiller capacity	10 kW
e	3.95614	COP-rated conditions	1.81
se	1.19813	Hot water flow rate	510 kg/hr
re	–76.91607	Cooling water flow rate	3170 kg/hr
sg	0.54388	Chilled water flow rate	1950 kg/hr
rg	–25.95760	Cp water	4.19 kJ/kgK

The thermal load data was scaled to fit the chiller size. To satisfy wide variations in cooling demand, the chiller was allowed to work between 20 and 140% of its nominal capacity. The simulations used water as the working fluid in the chiller loop.

3. System control

This system used three controllers, as described below. The solar and back-up systems are activated to fulfil the load and temperature requirements of the chiller. The simulations used fixed temperatures for the chilled water inlet (7 °C) and cooling water inlet (32 °C).

3.1. Collector control

The collector is activated by a controller. The first control approach modulates the pump mass flow rate to match a collector outlet set-point temperature (210 °C), which is the rated hot water temperature inlet condition for the chiller. The second control approach (known as hysteresis controller) operates the pump in an on/off mode. Depending on the temperature difference between the collector and the tank, the controller turns the pump on ($T_{coll,out} - T_{tank,bottom} > 15$ K) or off ($T_{coll,out} - T_{tank,bottom} < 5$ K). The controller system activates the collector only when the sun's radiation is higher than 150 W/m^2 during working days.

3.2. Tank, back-up and bypass control

The tank controller, which is based on two temperature sensors positioned at heights of 25% from the top and bottom locations, switches the back-up burner on or off. In the parallel configuration (shown in Figure 1), the tank is completely decoupled from the back-up heat source. In this configuration the chiller is supplied, at any given time, with either heat from the tank or heat from the burner. In the series configuration, the tank is always discharged, and the burner is switched on only if the fluid is not hot enough. Thus heat comes simultaneously from both solar and gas.

In both configurations, the controller operates a bypass valve to regulate the recirculated flow rate and obtain the requested chiller supply temperature.

3.3. Chiller control

The absorption chiller is activated when the building requires cooling. A controller in the cooling tower controls the fan speed to maintain a temperature of 32 °C at the chiller inlet. As described above, chiller cooling capacity is regulated by varying the generator supply water temperature.

4. Results

In order to investigate the system performance for different control configurations, and the influence of different system design parameters (e.g. storage volume, collector area), a parametric study has been carried out. The system was simulated for 80 scenarios, using combinations of four collector area values, five storage tank volumes, two collector controllers and two back-up burner system configurations.

The analysed parameters are the solar fraction (ratio between the solar heat to the total heat used by the system) and the collector yield (collected energy per unit of collector area). Storage volume is represented as residence time (ratio of tank volume to the chiller flow).

The results are shown in Figures 2–4. The annual solar fraction for various storage sizes and collector areas when using a hysteresis controller is shown in Figure 2. As expected, the solar fraction rises as collector area increases. For a given Specific collector Area (SA) in m^2 per kW of chiller capacity, the solar fraction falls as storage volume increases. This is attributed to greater heat losses from larger storage tanks. Figure 3 shows that tank losses increase about eight times due to a 30x increase in storage volume. This stresses the importance of choosing the correct insulation for high-temperature solar-cooling systems.

The effect of back-up burner positioning in the overall system layout can also be seen in the Figure 2. Parallel positioning of the back-up heat source results in a higher solar fraction, which is evident for large storage tank volumes. Analysis of component-level heat contribution shows the solar collector provides nearly similar heat to the system for series and parallel burner positioning. However, tank heat losses from a parallel positioned configuration are less, due to decoupling of the tank from the back-up heat source. For example, in the operating case with 0.615 specific collector area and 300 min storage residence time, tank heat loss for a series configuration was nearly twice that of a parallel back-up configuration. The mean tank temperature was also nearly 20 °C higher for a series back-up heating configuration.

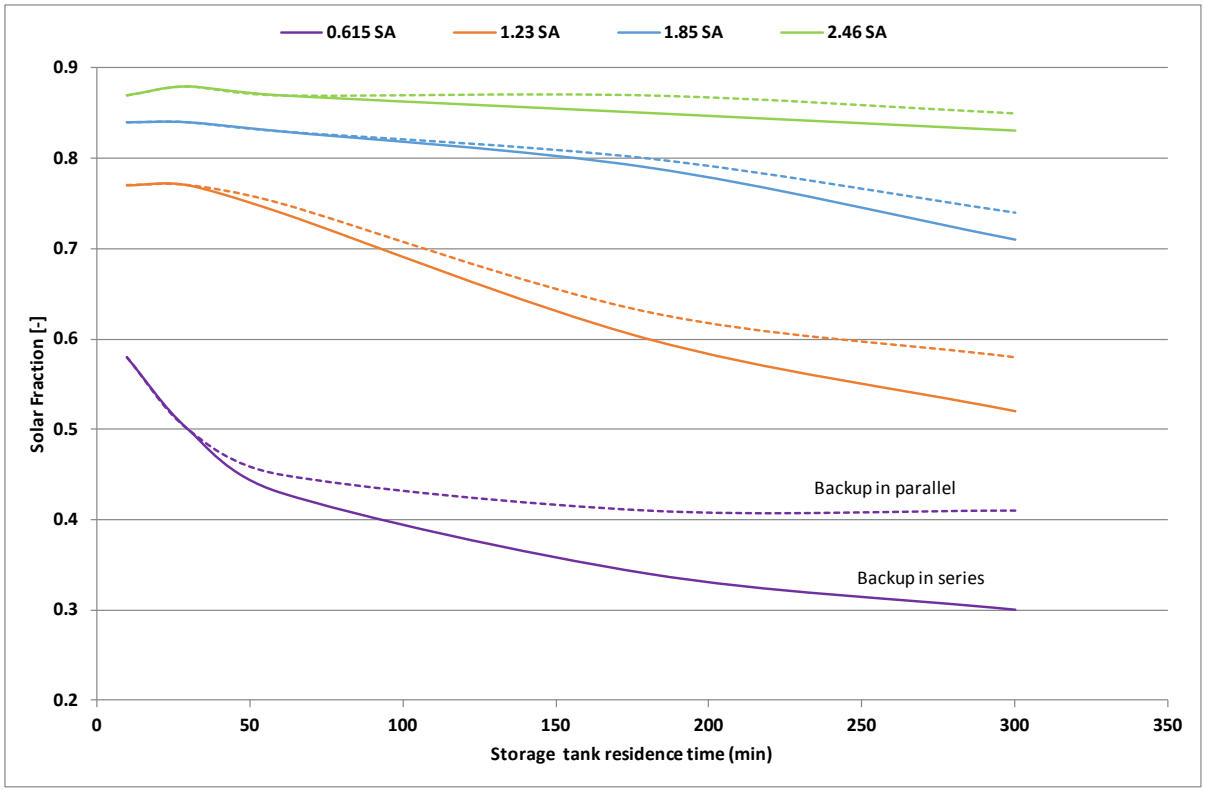

Figure 2. Solar fraction variation for different collector areas and storage volumes while employing a hysteresis controller

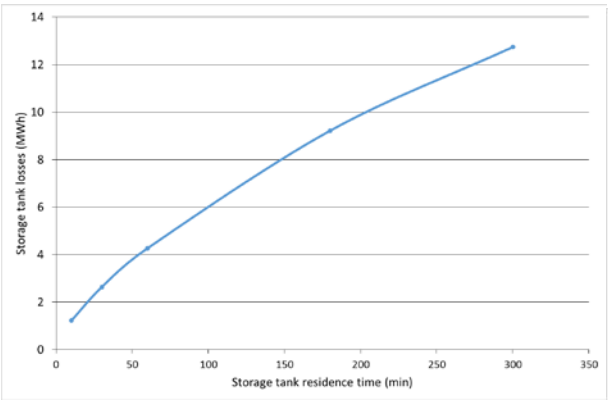

Figure 3. Effect of storage volume on heat losses: hysteresis controller, back-up in series.

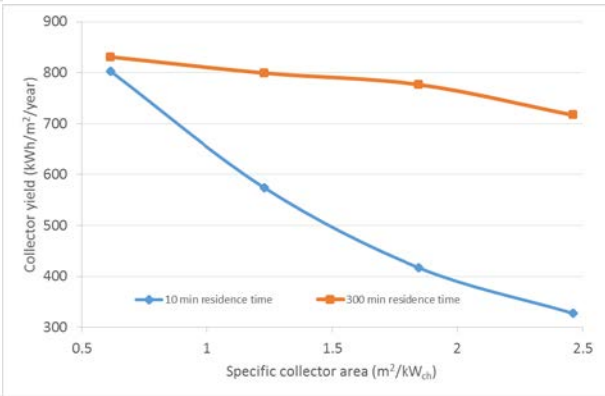

Figure 4. Influence of specific collector area on collector yield: hysteresis controller, back-up in series.

Figure 4 shows the effect of collector area and storage tank volume on collector yield. Collector yield falls as collector area increases for all storage tank volumes. This trend is due to the hysteresis control strategy, which places no restriction on the collector outlet temperatures. This results in higher temperature output for larger solar collector area values; the collector outlet temperature is >250 °C for a specific collector area of 1.85 or above. The high collector fluid temperatures make the collector less efficient, thereby decreasing collector yield. This trend is similar to the results obtained by Eicker and Pietruschka (2009) for an evacuated-collector, single-effect chiller-based solar air-conditioning system. Reduction in collector yield is more pronounced for smaller storage tanks than for larger tanks. Larger tanks have lower collector inlet temperatures, resulting in lower collector losses.

Figure 5 shows the effect of backup heat configuration, tank volume and collector size on solar fraction while using a temperature controller. During operation of this control, a variable speed pump alters the flow rate through the collector to maintain a fixed set point temperature at collector outlet. Comparison of this control strategy with hysteresis control strategy shows higher solar fraction obtained by this controller for higher specific collector area values. This controller is able to generate solar fractions higher than 0.9. Collector outlet temperature set point values closer to chiller requirements results in higher tank outlet temperatures for the temperature controller driven systems. As a result, the backup burner is less utilized to meet the cooling load resulting in higher solar fractions.

5. Conclusions

A high-temperature solar-cooling system with triple effect absorption chiller for an office building has been studied using system-level simulations. Characteristic equations approach has been used to model the performance of a triple effect chiller. Eighty test cases have been used to study the influence of collector size, storage size, control strategy and backup burner positioning on annual solar fraction. These results indicate that the solar collector outlet temperature control strategy with parallel gas backup configuration, provides higher solar fractions. Though the effect of collector area on the collector yield is similar to previous studies of single effect chiller based systems, these studies have shown tank heat losses play a more significant role in deciding annual solar fraction for high temperature solar cooling systems.

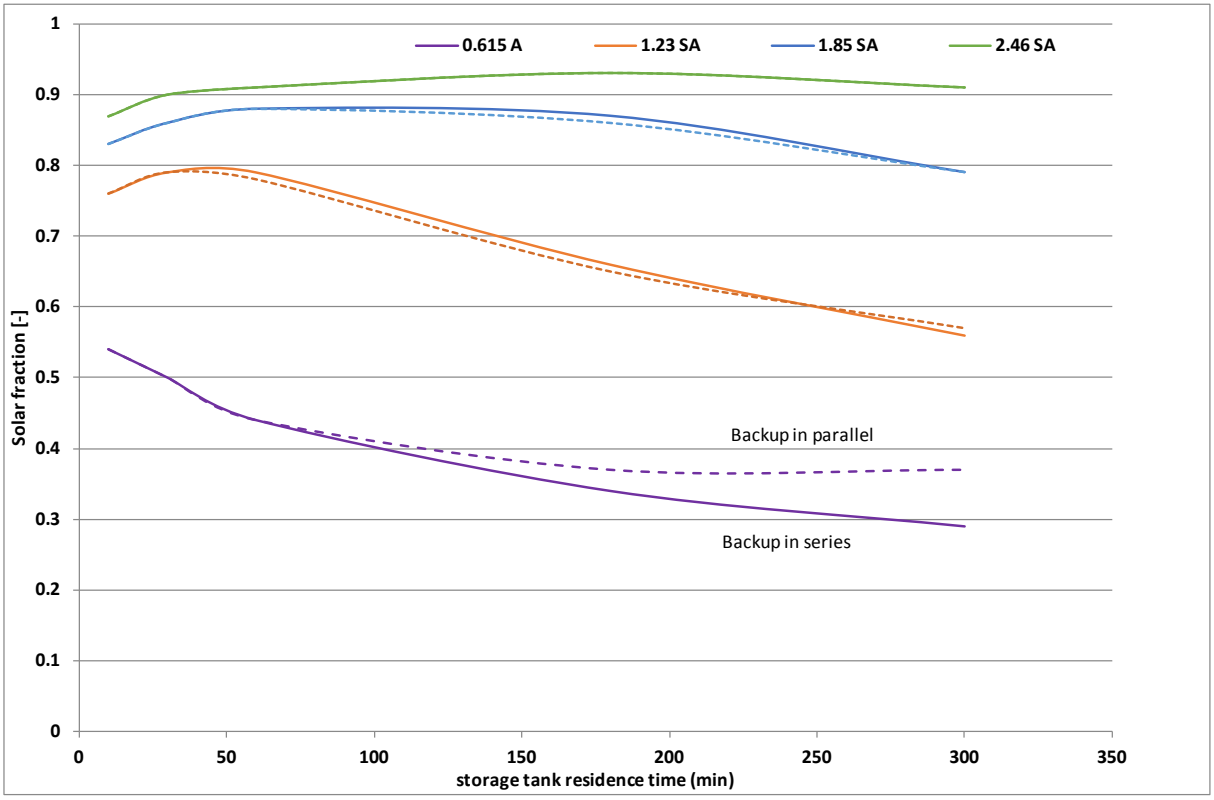

Figure 5. Solar fraction variation for different collector areas and storage volumes while employing a temperature controller

References

Al-Alili, a., Islam, M.D., Kubo, I., Hwang, Y., Radermacher, R., 2012, 'Modeling of a solar powered absorption cycle for Abu Dhabi', *Appl. Energy*, 93, p160–167.

Eicker, U., Pietruschka, D., 2009, 'Design and performance of solar powered absorption cooling systems in office buildings', *Energy Build.*, 41, p81–91.

Hang, Y., Du, L., Qu, M., Peeta, S., 2013, 'Multi-objective optimization of integrated solar absorption cooling and heating systems for medium-sized office buildings', *Renew. Energy*, 52, p67–78.

Kühn, A., Ziegler, F., 2005, 'Operational results of a 10 kW absorption chiller and adaptation of the characteristic equation', In: *Proceedings of the 1st International Conference on Solar Air Conditioning*, Bad-Staffelstein, Germany.

Labus, J., Bruno, J.C., Coronas, A., 2013, 'Performance analysis of small capacity absorption chillers by using different modeling methods', *Appl. Therm. Eng.*, 58, p305–313.

Mateus, T., Oliveira, A.C., 2009, 'Energy and economic analysis of an integrated solar absorption cooling and heating system in different building types and climates', *Appl. Energy*, 86, p949–957.

Pintaldi, S., Perfumo, C., Sethuvenkatraman, S., White, S., Rosengarten, G., 2015, 'A review of thermal energy storage technologies and control approaches for solar cooling', *Renew. Sustain. Energy Rev.*, 41, p975–995.

Puig-Arnavat, M., López-Villada, J., Bruno, J.C., Coronas, A., 2010, 'Analysis and parameter identification for characteristic equations of single- and double-effect absorption chillers by means of multivariable regression', *Int. J. Refrig.*, 33, p70–78.

Qu, M., Yin, H., Archer, D.H., 2010, 'A solar thermal cooling and heating system for a building: Experimental and model based performance analysis and design', *Sol. Energy*, 84, p166–182.

Solar Energy Laboratory, University of Wisconsin, M., 2011, TRNSYS 17, 'A Transient Simulation Program'.

Thermax, CSIRO, 2014, 'Private communication with Thermax in March 2014'.

Tsoutsos, T., Aloumpi, E., Gkouskos, Z., Karagiorgas, M., 2010, 'Design of a solar absorption cooling system in a Greek hospital', *Energy Build.*, 42, p265–272.

Acknowledgments

The authors thank Thermax Limited for providing data for the triple-effect absorption chiller.